Functional characterization of AC5 gain-of-function variants: Impact on the molecular basis of ADCY5-related dyskinesia

TB Doyle[1], **MP Hayes**[1], **DH Chen**[4], **WH Raskind**[5,6,7], and **VJ Watts**[1,2,3]

[1]Purdue University, Medicinal Chemistry and Molecular Pharmacology, 575 Stadium Mall Drive, West Lafayette, IN. 47907

[2]Purdue Institute for Integrative Neuroscience, Hall for Discovery Learning - #399, 207 South Martin Jischke Drive, West Lafayette, IN. 47907

[3]Purdue Institute for Drug Discovery, 720 Clinic Drive, West Lafayette, IN. 47907

[4]University of Washington, Department of Neurology, Seattle, WA. 98195-7720, University of Washington

[5]Medicine and Medical Genetics

[6]Psychiatry and Behavioral Sciences, Seattle, WA. 98195-7720

[7]Geriatric Research, Education, and Clinical Center Veterans Administration Puget Sound, Veterans Health Care Center Seattle, WA. 98108

Abstract

Adenylyl cyclases are key points for the integration of stimulatory and inhibitory G protein-coupled receptor (GPCR) signals. Adenylyl cyclase type 5 (AC5) is highly expressed in striatal medium spiny neurons (MSNs), and is known to play an important role in mediating striatal dopaminergic signaling. Dopaminergic signaling from the D_1 expressing MSNs of the direct pathway, as well as the D_2 expressing MSNs of the indirect pathway both function through the regulation of AC5 activity, controlling the production of the 2nd messenger cAMP, and subsequently the downstream effectors. Here, we used a newly developed cell line that used Crispr-Cas9 to eliminate the predominant adenylyl cyclase isoforms to more accurately characterize a series of AC5 gain-of-function mutations which have been identified in ADCY5-related dyskinesias. Our results demonstrate that these AC5 mutants exhibit enhanced activity to $G\alpha_s$-mediated stimulation in both cell and membrane-based assays. We further show that the increased cAMP response at the membrane effectively translates into increased downstream gene transcription in a neuronal model. Subsequent analysis of inhibitory pathways show that the AC5

mutants exhibit significantly reduced inhibition following D_2 dopamine receptor activation. Finally, we demonstrate that an adenylyl cyclase "P-site" inhibitor, SQ22536 may represent an effective future therapeutic mechanism by preferentially inhibiting the overactive AC5 gain-of-function mutants.

Keywords

Adenylyl cyclase; AC5; cAMP; Dopamine; Dyskinesia

1. Introduction

In the central nervous system, neuromodulators elicit their effects predominantly through binding and activating G protein-coupled receptors (GPCRs) expressed on the cell surface. Receptor activation transduces the extracellular signal across the plasma membrane and regulates intracellular effector pathways through the activation of heterotrimeric G proteins. Membrane bound adenylyl cyclases (ACs) are one of the best-characterized G protein effectors, which catalyze production of the second messenger cAMP from ATP (1). ACs serve as key intersections for the integration of both stimulatory and inhibitory signals that initiate from GPCR activation.

Adenylyl cyclase signaling is a critical regulator of the diverse cortical and thalamic inputs that converge on striatal medium spiny neurons (MSNs), the principal neuron type of the striatum (2). Adenylyl cyclase type 5 (AC5) has been identified as the primary AC isoform expressed in MSNs, accounting for an estimated 80% of cAMP generated (3, 4). AC5 integrates signals from key receptors in striatal MSNs, such as the stimulatory D_1 dopamine (D_1R) and A_{2A} adenosine ($A_{2A}R$) receptors (5, 6). Conversely, AC5 is also specifically regulated by the inhibitory D_2 dopamine (D_2R) and M_4 muscarinic (M_4R) receptors which reduce cAMP production in striatal MSNs (4, 7, 8).

The initiation and control of movement by the striatum is dependent upon a complex system of neural circuitry and requires delicately balanced GPCR and adenylyl cyclase signaling (9). D_1R expressing MSNs of the direct pathway project to and inhibit the substantia nigra pars reticulata (SNr) to promote movement, whereas activation of the D_2R MSNs of the indirect striatopallidal pathway results in the suppression of movement (9, 10). The importance of maintaining this balance is highlighted by recent exome sequencing results that identified novel gain-of-function mutations in the gene coding for AC5 in patients with a movement disorder initially named "familial dyskinesia and facial myokymia (FDFM)" but presently referred to as ADCY5-related dyskinesia (MIM606703) since the phenotypic spectrum has been more extensively studied (11–14). This rare hyperkinetic movement disorder is characterized by early-onset paroxysmal dyskinesia, dystonia, chorea, and myoclonus, involving the limbs and/or trunk (14, 15). Initial *in vitro* functional studies have shown that the AC5 gain-of-function mutations cause a significant enhancement of cAMP production in response to β-adrenergic stimulation compared to wildtype AC5 (13). While at least 15 disease-causing AC5 mutations have been identified in patients, the molecular mechanisms by which AC5 gain-of-function mutations translate to hyperkinetic movement

disorders remains unknown, increasing the difficulty to effectively treat patients to manage their symptoms (15, 16). Current pharmacological therapies vary widely, ranging from benzodiazapines and barbiturates to carbidopa-levodopa with limited effectiveness (15). Here, we took advantage of a newly developed HEK cell line that used Crispr-Cas9 to eliminate AC3 and AC6, the two most abundant endogenous ACs in HEK cells to reduce the background AC activity and cAMP signal (17). Using this novel cell model, we examined the functional characteristics of five AC5 mutations identified in patients with ADCY5-related dyskinesia, and further explore AC5 as a potential therapeutic target for this early-onset pleiotropic movement disorder.

2. Materials and Methods

Cell culture:

Both human embryonic kidney (HEK) 293 cells and stable CRISPR/Cas9 AC3 and AC6 knockout HEK cells (HEK-AC 3/6) were cultured in Dulbecco's Modified Eagle Medium (Life Technologies, Grand Island, NY), supplemented with 5% bovine calf serum (Hyclone, Logan, UT), 5% fetal clone I (Hyclone, Logan, UT), and 1% Antibiotic-Antimycotic 100x solution (Life Technologies, Grand Island, NY) as described previously (17). Cath a. differentiated (CAD) cells were cultured in Dulbecco's Modified Eagle Medium, supplemented with 5% bovine calf serum, 5% fetal bovine serum (Hyclone, Logan, UT), and 1% Antibiotic-Antimycotic 100x solution.

AC5 wildtype, R418W, R418Q, A726T, M1029K, and K694_M696del (9bp) constructs were cloned into the eGFP-N vector as described previously (13). For transient transfections, cells were seeded in 6-well culture dishes containing culture media, then incubated at 37°C and 5% CO_2 overnight to a confluency of 80%. 1.5 μg of the AC isoform plasmid DNA was transfected per well using Lipofectamine 2000 following the manufacturer's protocol. 1 μg D_{2L} dopamine receptor plasmid DNA or 1 μg CRE-pGL3 luciferase reporter plasmid DNA was additionally co-transfected for select experiments. Twenty-four hours following the transfection, media was aspirated and replaced with culture media, before being returned to the incubator overnight. Forty-eight hours following transfection, cells were washed gently with warm phosphate buffered saline (PBS) and dissociated using non-enzymatic cell dissociation buffer (Gibco, Grand Island, NY). Cells were collected in a conical tube and pelleted by centrifugation at 500 xg for 5 minutes. The supernatant liquid was aspirated, and the cell pellet was re-suspended in warm OptiMEM (Gibco, Grand Island, NY) for assay.

Membrane Fraction Preparation and Assay:

HEK-AC 3/6 cells were grown and transiently transfected as described above. Culture media was aspirated and replaced with ice-cold lysis buffer (1mM HEPES, 2mM EDTA, pH 7.4) and incubated on ice for 15 minutes. Cells were scraped from the plate using sterile scrapers, collected, suspended in lysis buffer, and triturated by pipetting. Cells were centrifuged at 30,000 xg for 20 minutes at 4°C. The supernatant was discarded, and the remaining pellet resuspended in receptor binding buffer (4 mM $MgCl_2$, 50 mM Tris, pH 7.4). The cell membrane resuspension was homogenized using a Kinematica homogenizer (Kinematica, Switzerland) and aliquotted in 1 ml fractions. After the aliquots were

centrifuged at 12,000 xg for 10 minutes at 4°C, the supernatant removed by aspiration, and the remaining membrane pellet was frozen at −80 °C until use.

Briefly, AC membrane aliquots were thawed on ice and resuspended in membrane buffer (33 mM HEPES, pH 7.4, 0.5 mM EGTA, 0.1% Tween20). A BCA assay was used to determine the protein concentration for each sample, which were diluted to 25 μg/ml. Diluted membranes were plated into a white, flat bottom, tissue culture-treated 384 well plate (PerkinElmer, Shelton, CT) at 10 μl/well, and briefly centrifuged. An additional 5 μl/well of membrane buffer was added to the appropriate wells. Activated $G\alpha_s$ was diluted in stimulation buffer (33 mM HEPES, pH 7.4, 10 mM $MgCl_2$, 1 mM ATP, 4 μM GTPγS, 0.1% Tween20, 2 mM IBMX), and 5 μl added to each appropriate well. The plate was briefly centrifuged and incubated at room temperature for 1 hour before addition of Cisbio HTRF cAMP detection reagents and cAMP measurement as described further below.

CRE-Luciferase Assay:

Cath a. Differentiated (CAD) cells were transiently transfected as described above. Based on GFP-fusion proteins, we typically see modest expression efficiencies between 50–70% with adenylyl cyclases. Twenty-four hours following transfection, cell culture media was aspirated, and cells were dissociated using non-enzymatic cell dissociation buffer and centrifuged at 500 xg for 5 minutes. The supernatant was discarded, and cell pellet resuspended and diluted in OptiMEM buffer. 20 μl/well of the diluted cell suspension was plated into a white, flat bottom, tissue culture-treated 384 well plate (PerkinElmer, Shelton, CT), then briefly centrifuged before being stored in a humidified incubator at 37°C and 5% CO_2 for 24 hours. To stimulate the endogenously expressed $G\alpha_s$-coupled adenosine A_{2A} receptors on CAD cells, 10 μl/well of the A_{2A} receptor agonist CGS 21680 was added (1 μM final concentration), and the plate was briefly centrifuged and then incubated at 37°C with 5% CO_2 for 3 hours. Steadylite plus (PerkinElmer, Shelton, CT) luciferase reagent was added according to manufacturer's instructions, and luminescence measured using a Synergy Neo2 (BioTek, Winooski, VT).

Cisbio HTRF cAMP Assay:

cAMP accumulation was measured using the Cisbio HTRF cAMP dynamic-2 assay kit according to the manufacturer's instructions. Following aspiration of culture media from plates containing transfected cells, they were gently washed with warm PBS and treated with non-enzymatic cell dissociation buffer. Cell suspensions were centrifuged at 500 xg for 5 minutes, supernatant aspirated, and cell pellets resuspended in warm OptiMEM buffer. Cells were diluted as indicated and 10 μl/well plated into a white, flat bottom, tissue culture-treated 384-well plate (PerkinElmer, Shelton, CT). Assay plates containing live cells were briefly centrifuged at 100 xg for 30 seconds and incubated in a humidified incubator at 37°C and 5% CO_2 for 1 hour before further treatment.

Acute cAMP accumulation was measured by adding 10 μl/well isoproterenol or prostaglandin E2 (PGE2) to stimulate endogenously expressed $G\alpha_s$ coupled GPCRs, or 5 μl/ well forskolin (FSK) to stimulate the adenylyl cyclase directly, in OptiMEM containing 3-isobutyl-1-methylxanthine (IBMX) 500 μM final concentration. Plates were briefly

centrifuged, then incubated at room temperature for 1 hour before cell lysis and measurement of cAMP accumulation. Assay plates were excited using 330 nm wavelength, and fluorescent emission at 620 nm and 665 nm was analyzed using a Synergy Neo2 (BioTek, Winooski, VT). Ratiometric analyses were performed with GraphPad Prism (GraphPad Software, La Jolla, CA) by dividing the 665nm emission by the 620nm emission to interpolate cAMP concentrations from a cAMP standard curve.

Acute cAMP inhibition experiments were conducted by adding 5 μl/well of either inhibitor or the D_2 agonist quinpirole, as specified. Plates were briefly centrifuged, incubated for 15 minutes at room temperature, then stimulated by adding 5 μl/well isoproterenol (1 μM final concentration) in IBMX to the wells. Plates were incubated for 1 hour at room temperature before cell lysis and cAMP measurement as described above.

Protein Expression and Purification:

$G\alpha_s$ was expressed as a N-terminally 6XHis tagged protein in BL21(DE3) *E. coli*, essentially as described previously (18). This protein has previously been shown to stimulate cAMP production in membrane fractions from cells over expressing AC5 (19). Colonies from a fresh transformation were selected and cultured at 37°C and 250 rpm in Terrific Broth until OD600 of 0.5 was reached, at which time cultures were induced with 30 μM IPTG and grown for 16 hrs at 18°C. Bacterial cells were pelleted at 1,000 x*g* and resuspended in Buffer A (25 mM HEPES, 5 mM $MgCl_2$, 150 mM NaCl, 5 mM β-mercaptoethanol, 20 μM GDP, pH 8) and supplemented with 1 mg/ml lysozyme and 0.01 mg/ml DNase I. Lysis was performed for 20 minutes on ice, and lysate was clarified by centrifugation at 30,000 xg. The supernatant was then subjected to immobilized metal affinity chromatography using 5 ml His-Pur Ni-NTA resin (Thermo Scientific, Waltham, MA) and eluted using Buffer A containing 200 mM imidazole and 1 mM NaCl. $G\alpha_s$-containing fractions were identified via SDS-PAGE, pooled, and further purified by ion exchange chromatography using a 1ml HiTrap Q Sepharose column (GE Healthcare, Chicago, IL) over a gradient of Buffer A containing 1 mM to 400 mM NaCl. $G\alpha_s$-His containing fractions were snap frozen in liquid nitrogen and stored at −80°C until use. Nucleotide exchange was performed in 50 mM HEPES, 2 mM DTT, 250 mM GTPγS, and 1 mM $MgCl_2$ for 20 minutes on ice, followed by 30 minutes at 30°C as described previously (19).

Western Blotting:

Unless otherwise listed, reagents were purchased from Thermo Fisher (Thermo Scientific, Waltham, MA). Anti-GFP antibody was purchased from Takara Bio (Kusatsu, Japan) and used at 1:1,000, anti-α tubulin antibody was purchased from Novus biological (Littleton, CO) and used at 1:5,000. Briefly, transfected cells were washed with ice cold PBS before being dissociated from the cell culture dish with non-enzymatic cell dissociation buffer and centrifuged at 800 xg for 5 minutes. The cell pellet or membrane fraction was re-suspended in lysis buffer containing 50 mM HEPES, pH 7.4, 150 mM NaCl, 1mM EDTA, 1 mM $MgCl_2$, 0.5% $C_{12}E_{10}$, 1 mM DTT, and protease inhibitor cocktail and incubated on ice for 30 minutes before being centrifuged at 18,000 xg at 4°C for 10 minutes to separate the insoluble fraction. Supernatant was transferred to a new Eppendorf tube, and protein

concentration determined by BCA assay. Protein samples were separated on 4–16% gradient gels and transferred to PVDF membrane. Membranes were blocked in 5% non-fat milk for 1 hour at room temperature, the membrane was probed for the protein of interest with primary antibodies diluted in TBST with 1% milk, by rocking overnight at 4°C. The membrane was washed with TBST, then incubated with a secondary IRDye 680RD anti-mouse or IRDye 800CW anti-rabbit at 1:10,000 for 1 hour at room temperature (LICOR Biotechnology, Lincoln, NE). Band intensities were quantified using ImageJ software (NIH, Bethesda, MD).

Data and Statistical Analyses:

All data and statistical analyses were carried out using GraphPad Prism 7 (GraphPad Software, San Diego, CA). Statistical analyses (one sample t tests, one-way ANOVAs) are described in text or figure legends where appropriate.

3. Results

AC5 mutants exhibit enhanced activity to $G\alpha_s$-mediated stimulation in cell-based assays

A previous study of two AC5 variants, R418W and A726T, showed significantly enhanced AC activity compared to wildtype in response to single point stimulation of 10 μM isoproterenol, consistent with a gain-of-function effect (13). The work presented here expands on these previous results by examining the specific signaling characteristics for five AC5 variants associated with ADCY5-related dyskinesia in the recently developed adenylyl cyclase knockout HEK293 cell line (13, 20). HEK-AC 3/6 cells lacking the predominant adenylyl cyclase isoforms AC3 and AC6 exhibit a 95% reduction in Fsk-stimulated cAMP accumulation (17). Furthermore, the cAMP response to isoproterenol and PGE_2 was shown to be reduced by > 75% and >85%, respectively (17). This cell line allows for the specific examination of the unique signaling characteristics of AC5 mutants, in the absence of cAMP accumulation caused by the most abundant endogenous AC isoforms.

To assess the activity of each AC5 mutant, HEK-AC 3/6 cells were transiently transfected with the respective AC5-eGFP tagged construct, and stimulation by two endogenous GPCRs and the small molecule allosteric activator FSK was assessed. We considered the possibility that the enhanced activity previously observed could be due to differences in signaling efficiency resulting from receptor localization within or outside of lipid rafts. We therefore examined the stimulatory effect of the non-lipid raft localized prostaglandin receptor (PGER) and the lipid raft localized β-adrenergic receptor (βAR) on AC5 mutants (21, 22). Activation of the prostaglandin receptor, with PGE_2 revealed that all five AC5 mutants exhibited significantly enhanced cAMP production compared to wildtype AC5 (Fig. 1A). At 10 μM PGE_2, the 9bp mutant showed the greatest cAMP accumulation compared to wildtype at 528±20%, followed by A726T (359±25%), R418W (344±49%), R418Q (277±38%), and M1029K (284±17%). Though each mutant showed changes in the efficacy of PGE_2, no significant differences in potency were observed (Table 1). These results were further corroborated through use of another endogenously expressed $G\alpha_s$ coupled receptor, the β-adrenergic receptor, which was activated with isoproterenol. Similarly, all five AC5 mutants exhibited significantly enhanced cAMP production in response to isoproterenol-mediated stimulation (Fig. 1B). At 10 μM isoproterenol, in comparison to wildtype AC5, the

Δ9bp mutant was again the most active with 492±19%, followed by R418W (332±51%), A726T (302±35%), R418Q (301±5%), and finally M1029K (241±18%). Similar to PGE_2, no significant differences in potency to isoproterenol were observed (Table 1). Following stimulation by 100 μM FSK, the most active mutant Δ9bp exhibited a significant increase in cAMP production compared to wildtype AC5 (142±14%) (Fig. 1C). FSK stimulation did not produce any significant difference in activity at 100 μM between the wildtype AC5 and the remaining four mutants tested. Matched cells from each transfection/assay were used for Western blotting to assess AC5 construct expression revealing no significant differences (Fig. 1D).

Purified $G\alpha_s$ reproduces exaggerated cAMP response observed with AC5 mutants in cell-free assay

The protein-protein interactions that make up macromolecular AC signaling complexes have been demonstrated to directly modulate acute AC5 activity (1, 23). To ensure that the enhanced activity associated with the gain-of-function AC5 mutations was the result of heightened enzymatic activity, rather than changes in intracellular signaling pathways, we examined two representative mutants in a cell-free assay. Membrane preparations of HEK-ACΔ3/6 cells transiently transfected with either AC5 R418W or A726T were stimulated with increasing concentrations of purified $G\alpha_s$ protein. Membranes containing R418W or A726T AC5 mutants exhibited robust and significantly enhanced cAMP production compared to membranes containing wildtype AC5 (Fig. 2). The R418W mutant increased cAMP production to 166±5% of wildtype AC5, while the A726T mutant exhibited 178±4%. As observed in living cells treated with PGE_2 or isoproterenol, no difference in the potency of purified $G\alpha_s$ was observed between wildtype AC5 and R418W or A726T. Matched membranes from each transfection/assay were used for Western blotting to assess construct expression and no significant differences were observed (Fig. 2B).

Increased cAMP response translates into increased downstream gene transcription in a neuronal cell model

In order to determine whether the enhanced activity of the AC5 mutant translated into downstream changes in gene transcription, we evaluated the ability of two representative AC5 mutants to activate transcription of a cAMP response element (CRE) luciferase reporter in a neuronal cell model. Cath a. Differentiated (CAD) cells transiently expressing the respective AC5 construct and the CRE-Luc reporter were treated with 1 μM CGS21680 to selectively activate endogenous A_{2A} adenosine receptors ($A_{2A}R$). Consistent with the previous functional data, the R418W and A726T mutants significantly increased downstream CRE-mediated transcription compared to wildtype AC5 (Fig. 3). $A_{2A}R$ stimulation increased relative luminescence of R418W and A726T expressing CAD cells by 164±3% and 147±2%, respectively, over cells expressing AC5 wildtype.

AC5 mutants exhibit significantly reduced inhibition following D_2 dopamine receptor activation

AC5 shows robust inhibition by $G\alpha_{i/o}$-coupled receptor activation (1). We therefore tested whether the AC5 mutations associated with gain-of-function activity affected $G\alpha_{i/o}$-mediated inhibition. HEK-ACΔ3/6 cells expressing the D_2 dopamine receptor (D_2R) and

respective AC5 constructs were treated with the D_2R selective agonist quinpirole, and then stimulated with 1 μM isoproterenol. Wildtype AC5 exhibited a robust inhibition of 96±4% in response to D_2R activation. Interestingly, D_2-mediated inhibition of all five AC5 mutants was significantly blunted compared to AC5 WT (Fig. 4). Isoproterenol stimulated activity of the R418W mutant was reduced to 50±3% at 10 μM quinpirole; followed by M1029K at 52±4%, 9bp at 54±5%, A726T at 59±2%, and R418Q at 64±2%. No significant change in quinpirole potency between AC5 WT and the five mutants was observed (Table 1).

P-site inhibitors preferentially inhibit overactive AC5 mutants

P-site inhibitors are a class of AC inhibitors that bind the transition state of the enzyme, preventing the formation of cAMP. This class of inhibitors are activity dependent; as the enzyme activity increases, more transition states are available for inhibition (24). We therefore assessed the ability of SQ 22,536 to inhibit isoproterenol stimulated AC5 activity. SQ 22,536 inhibited the five AC5 mutants to a significantly greater degree compared to wildtype (Fig. 5). Similar results were obtained with each mutant, with inhibition ranging from 88±1% for the 9bp mutant (highest inhibition) to 84±1% for A726T (lowest inhibition), compared to 53±6% inhibition of wildtype AC5. No significant differences in potency were observed between the mutants and wildtype AC5 (Table 1).

4. Discussion

With advances in sequencing technology, there has been considerable progress in understanding the molecular etiology for rare and neglected diseases. Whole exome sequencing of patients with a previously unspecified dyskinesia resulted in the identification of a series of variants in the gene for AC5. Identification of these mutations provided a foundation by which to expand our scientific knowledge of G protein-coupled receptor (GPCR) signal transduction, with the ultimate goal of improving medical treatment for patients with ADCY5-related dyskinesia. In this study, we further expand on existing research by functionally characterizing five disease-related AC5 mutations. Our use of a recently developed HEK cell line that lacks the predominant AC isoforms allowed for a highly focused analysis of the unique signaling characteristics of each AC5 variant with an enhanced signal-to-noise ratio (17). All five variants studied demonstrated enhanced activity with respect to accumulation of cAMP when stimulated via either the dopaminergic or beta-adrenergic pathways.

To investigate how different populations of endogenously expressed stimulatory GPCRs affect adenylyl cyclase activity, we examined whether lipid raft localized receptors exhibited differences in signaling efficiency with these five mutations. Areas of the lipid bilayer have been demonstrated to form specialized microdomains, known as lipid rafts, which promote the assembly of signaling complexes and facilitate the formation of efficient GPCR signaling complexes (1, 25). We compared the ability of prostaglandin receptors (PGERs), which typically do not associate in lipid rafts, with the lipid raft localized β-adrenergic receptors to stimulate AC5 activity (1). The results indicate that stimulation by both receptor subtypes elicited a significantly enhanced cAMP response from the five AC5 mutants compared to wildtype, suggesting that lipid raft localization of $G\alpha_s$-coupled receptors does not play a

substantial role in the enhanced stimulatory signaling observed with the five ADCY5-related dyskinesia causative gain-of-function mutants. Through the use of isolated cell membranes and purified $G\alpha_s$ protein, we demonstrate that two recurrent AC5 mutants, R418W and A726T, displayed significantly increased cAMP accumulation compared to wildtype AC5 in response to $G\alpha_s$-mediated stimulation. Together, these observations suggest that the enhanced cAMP production associated with the AC5 gain-of-function mutations in cell-based assays is the result of increased responsiveness to $G\alpha_s$-stimulated enzymatic activity.

To further understand how enhanced cAMP production at the cell membrane influences downstream effectors, we examined the effect of the two representative AC5 gain-of-function mutants on cAMP response element (CRE)-mediated gene transcription in a neuronal cell model. CRE activation is the final step in a signal transduction cascade, which is initiated by adenylyl cyclase stimulation. The subsequent increase in cAMP production promotes the dissociation and activation of protein kinase A catalytic subunits, which translocate into the nucleus and phosphorylate a number of proteins, including the cAMP response element binding protein (CREB) to stimulate transcription. Cath. a differentiated (CAD) cells endogenously express multiple adenylyl cyclase isoforms, as indicated by the increase of luminescence from control vector expressing cells in response to A_{2A} adenosine receptor-mediated stimulation. Despite the elevated background, CAD cells expressing the R418W or A726T AC5 mutation displayed significantly higher CRE-mediated gene transcription compared to wildtype AC5 expressing cells. Gene transcription in neuronal cells is a tightly regulated event (26). These results therefore indicate that the enhanced cAMP production observed with the AC5 gain-of-function mutations is not limited to membrane localized effects, but rather their activity can permeate downstream effector pathways to elicit global effects.

Presently, our knowledge regarding the structure and functional regulation of the catalytic domains of mammalian adenylyl cyclases is largely based upon X-ray structural analysis of recombinant catalytic domains (1, 27). This structure indicates that none of the five mutations studied here occur in the catalytic site or at the interface with $G\alpha_s$ (27). Furthermore, the mutated residues are not directly involved in the coordination of substrate, product, metal ions, or the allosteric activator forskolin within the catalytic site (1, 27). Rather, modeling places these mutations at the juxtamembrane junction between membrane spanning helices and the cytosolic regions responsible for catalysis (1). Bacterial adenylyl cyclase crystal structures suggest that these regions are likely helical and may function to regulate C1 and C2 catalytic domain interactions (28). $G\alpha_s$ stimulation of adenylyl cyclase promotes the stabilization of the C1 and C2 domains to form catalytically active pseudo-heterodimers, as well as the loops and structural features that support catalysis (1, 27). Therefore, it seems likely that the AC5 gain-of-function mutations facilitate the interaction of the C1 and C2 catalytic domains in response to binding of $G\alpha_s$, which promotes enhanced cAMP production. However, this possible mechanism is complicated by similar responsiveness to direct activation by high concentrations of FSK, as well as differences in potency for some of the mutants (Table 1). This complicated relationship between $G\alpha_s$ and FSK responsiveness is consistent with previous studies examining AC5 mutations that resulted in reduced $G\alpha_s$ sensitivity, while simultaneously producing a wide range of FSK

sensitivity, suggesting possibly independent mechanisms for activation by these classical agents (29, 30).

AC5 is characteristically sensitive to $G\alpha_{i/o}$-mediated inhibition; we therefore examined how the activation of the D_2 dopamine receptor (D_2R) effected $G\alpha_s$-mediated stimulation (1, 31). Our results indicate that selective activation of D_2R robustly inhibits wildtype AC5, however the maximal inhibition of all five AC5 gain-of-function mutants was significantly blunted. These results indicate that not only do the mutant cyclases respond more robustly to $G\alpha_s$-mediated stimulation, they are also appear more weakly inhibited by $G\alpha_{i/o}$-coupled receptors, potentially further shifting the delicate balance of intracellular cAMP signaling within the neural circuitry of the striatum. As previously described, the striatum is a principal input structure of the basal ganglia and receives neurological input from the motor cortex; which is dynamically controlled with the support of the direct and indirect striatal output pathways to provide opposing influence on the initiation and maintenance of movement (9, 10). Our results suggest that patients expressing AC5 gain-of-function mutations may have enhanced direct pathway activity, in combination with reduced disinhibition from the D_2R-mediated indirect pathway. This loss of cooperative activity in both direct and indirect pathways likely results in an unsynchronized enhancement of movement initiation (Fig. 6).

Despite the increasing awareness of ADCY5-related dyskinesia, treatments available for patients remain limited and are not specific for the pathogenesis of the disorder (15). While barbiturates and benzodiazepines are commonly prescribed for them and can be of benefit especially at night, dopamine receptor agonists in the form of carbidopa-levodopa have also been used with limited success (15). The mechanism for the enhanced activity of the AC5 mutants may suggest a more targeted therapeutic. As predicted by previous studies (9, 10), we observed that a P-site inhibitor had an enhanced effect at the AC5 gain-of-function mutants compared to wildtype. Because P-site inhibitors bind to the catalytic pocket and mimic a cAMP-bound transition state, increased enzyme activity results in a more inaccessible conformation, essentially selectively targeting the most active enzymes (24). Unfortunately, the only FDA approved P-site inhibitor, Vidarabine, lacks AC5 selectivity and would presumably have significant negative side effects (32). Evidence has demonstrated that diminished AC5 signaling is associated with detrimental side effects, and therefore the development of an activity-independent AC5 inhibitor draws statements of caution (4). However, because of the unique mechanism of action of P-site inhibitors, we hope that the further development of more potent and isoform selective P-site inhibitors could be applied to ADCY5 dyskinesias and other clinically relevant conditions.

Funding:

Abbreviations:

AC   Adenylyl cyclase

AC5	Adenylyl cyclase type 5
cAMP	3',5'-cyclic adenosine monophosphate
DA	Dopamine
FSK	Forskolin
GPCR	G protein coupled-receptor
PGE2	Prostaglandin E2
MSN	striatal medium spiny neuron

References:

1. Dessauer CW, Watts VJ, Ostrom RS, Conti M, Dove S, Seifert R. International Union of Basic and Clinical Pharmacology. CI. Structures and Small Molecule Modulators of Mammalian Adenylyl Cyclases. Pharmacol Rev. 2017;69(2):93–139. doi: 10.1124/pr.116.013078. PubMed PMID: 28255005; PMCID: PMC5394921. [PubMed: 28255005]

2. Tepper JM, Bolam JP. Functional diversity and specificity of neostriatal interneurons. Curr Opin Neurobiol. 2004;14(6):685–92. doi: 10.1016/j.conb.2004.10.003. PubMed PMID: 15582369. [PubMed: 15582369]

3. Pieroni JP, Miller D, Premont RT, Iyengar R. Type 5 adenylyl cyclase distribution. Nature. 1993;363(6431):679–80. doi: 10.1038/363679a0. PubMed PMID: 8515810. [PubMed: 8515810]

4. Lee KW, Hong JH, Choi IY, Che Y, Lee JK, Yang SD, Song CW, Kang HS, Lee JH, Noh JS, Shin HS, Han PL. Impaired D2 dopamine receptor function in mice lacking type 5 adenylyl cyclase. The Journal of neuroscience : the official journal of the Society for Neuroscience. 2002;22(18):7931–40. PubMed PMID: 12223546. [PubMed: 12223546]

5. Herve D Identification of a specific assembly of the g protein golf as a critical and regulated module of dopamine and adenosine-activated cAMP pathways in the striatum. Front Neuroanat. 2011;5:48. doi: 10.3389/fnana.2011.00048. PubMed PMID: 21886607; PMCID: PMC3155884. [PubMed: 21886607]

6. Corvol JC, Studler JM, Schonn JS, Girault JA, Herve D. Galpha(olf) is necessary for coupling D1 and A2a receptors to adenylyl cyclase in the striatum. Journal of neurochemistry. 2001;76(5):1585–8. PubMed PMID: 11238742. [PubMed: 11238742]

7. Sanchez G, Colettis N, Vazquez P, Cervenansky C, Aguirre A, Quillfeldt JA, Jerusalinsky D, Kornisiuk E. Muscarinic inhibition of hippocampal and striatal adenylyl cyclase is mainly due to the M(4) receptor. Neurochem Res. 2009;34(8):1363–71. doi: 10.1007/s11064-009-9916-9. PubMed PMID: 19191026. [PubMed: 19191026]

8. Nair AG, Gutierrez-Arenas O, Eriksson O, Vincent P, Hellgren Kotaleski J. Sensing Positive versus Negative Reward Signals through Adenylyl Cyclase-Coupled GPCRs in Direct and Indirect Pathway Striatal Medium Spiny Neurons. The Journal of neuroscience : the official journal of the Society for Neuroscience. 2015;35(41):14017–30. doi: 10.1523/JNEUROSCI.0730-15.2015. PubMed PMID: 26468202; PMCID: PMC4604235.

9. Haber SN. The place of dopamine in the cortico-basal ganglia circuit. Neuroscience. 2014;282:248–57. doi: 10.1016/j.neuroscience.2014.10.008. PubMed PMID: 25445194; PMCID: PMC5484174. [PubMed: 25445194]

10. Bordia T, Perez XA. Cholinergic control of striatal neurons to modulate L-dopa-induced dyskinesias. Eur J Neurosci. 2018. doi: 10.1111/ejn.14048. PubMed PMID: 29923650.

11. Fernandez M, Raskind W, Wolff J, Matsushita M, Yuen E, Graf W, Lipe H, Bird T. Familial dyskinesia and facial myokymia (FDFM): a novel movement disorder. Annals of neurology. 2001;49(4):486–92. PubMed PMID: 11310626. [PubMed: 11310626]

12. Chen YZ, Matsushita MM, Robertson P, Rieder M, Girirajan S, Antonacci F, Lipe H, Eichler EE, Nickerson DA, Bird TD, Raskind WH. Autosomal dominant familial dyskinesia and facial

myokymia: single exome sequencing identifies a mutation in adenylyl cyclase 5. Arch Neurol. 2012;69(5):630–5. doi: 10.1001/archneurol.2012.54. PubMed PMID: 22782511; PMCID: PMC3508680. [PubMed: 22782511]

13. Chen YZ, Friedman JR, Chen DH, Chan GC, Bloss CS, Hisama FM, Topol SE, Carson AR, Pham PH, Bonkowski ES, Scott ER, Lee JK, Zhang G, Oliveira G, Xu J, Scott-Van Zeeland AA, Chen Q, Levy S, Topol EJ, Storm D, Swanson PD, Bird TD, Schork NJ, Raskind WH, Torkamani A. Gain-of-function ADCY5 mutations in familial dyskinesia with facial myokymia. Annals of neurology. 2014;75(4):542–9. doi: 10.1002/ana.24119. PubMed PMID: 24700542; PMCID: PMC4457323. [PubMed: 24700542]

14. Chen DH, Meneret A, Friedman JR, Korvatska O, Gad A, Bonkowski ES, Stessman HA, Doummar D, Mignot C, Anheim M, Bernes S, Davis MY, Damon-Perriere N, Degos B, Grabli D, Gras D, Hisama FM, Mackenzie KM, Swanson PD, Tranchant C, Vidailhet M, Winesett S, Trouillard O, Amendola LM, Dorschner MO, Weiss M, Eichler EE, Torkamani A, Roze E, Bird TD, Raskind WH. ADCY5-related dyskinesia: Broader spectrum and genotype-phenotype correlations. Neurology. 2015;85(23):2026–35. doi: 10.1212/WNL.0000000000002058. PubMed PMID: 26537056; PMCID: PMC4676753. [PubMed: 26537056]

15. Dy ME, Chang FC, Jesus SD, Anselm I, Mahant N, Zeilman P, Rodan LH, Foote KD, Tan WH, Eskandar E, Sharma N, Okun MS, Fung VS, Waugh JL. Treatment of ADCY5-Associated Dystonia, Chorea, and Hyperkinetic Disorders With Deep Brain Stimulation: A Multicenter Case Series. J Child Neurol. 2016;31(8):1027–35. doi: 10.1177/0883073816635749. PubMed PMID: 27052971. [PubMed: 27052971]

16. Carecchio M, Mencacci NE, Iodice A, Pons R, Panteghini C, Zorzi G, Zibordi F, Bonakis A, Dinopoulos A, Jankovic J, Stefanis L, Bhatia KP, Monti V, R'Bibo L, Veneziano L, Garavaglia B, Fusco C, Wood N, Stamelou M, Nardocci N. ADCY5-related movement disorders: Frequency, disease course and phenotypic variability in a cohort of paediatric patients. Parkinsonism Relat Disord. 2017;41:37–43. doi: 10.1016/j.parkreldis.2017.05.004. PubMed PMID: 28511835; PMCID: PMC5549507. [PubMed: 28511835]

17. Soto-Velasquez M, Hayes MP, Alpsoy A, Dykhuizen EC, Watts VJ. A Novel CRISPR/Cas9-Based Cellular Model to Explore Adenylyl Cyclase and cAMP Signaling. Molecular pharmacology. 2018;94(3):963–72. doi: 10.1124/mol.118.111849. PubMed PMID: 29950405; PMCID: PMC6064782. [PubMed: 29950405]

18. Lee E, Linder ME, Gilman AG. Expression of G-protein alpha subunits in Escherichia coli. Methods Enzymol. 1994;237:146–64. PubMed PMID: 7934993. [PubMed: 7934993]

19. Chen-Goodspeed M, Lukan AN, Dessauer CW. Modeling of Galpha(s) and Galpha(i) regulation of human type V and VI adenylyl cyclase. The Journal of biological chemistry. 2005;280(3):1808–16. doi: 10.1074/jbc.M409172200. PubMed PMID: 15545274. [PubMed: 15545274]

20. Douglas AG, Andreoletti G, Talbot K, Hammans SR, Singh J, Whitney A, Ennis S, Foulds NC. ADCY5-related dyskinesia presenting as familial myoclonus-dystonia. Neurogenetics. 2017;18(2):111–7. doi: 10.1007/s10048-017-0510-z. PubMed PMID: 28229249; PMCID: PMC5359383. [PubMed: 28229249]

21. Ostrom RS, Insel PA. The evolving role of lipid rafts and caveolae in G protein-coupled receptor signaling: implications for molecular pharmacology. British journal of pharmacology. 2004;143(2):235–45. doi: 10.1038/sj.bjp.0705930. PubMed PMID: 15289291; PMCID: PMC1575337. [PubMed: 15289291]

22. Ostrom RS, Bogard AS, Gros R, Feldman RD. Choreographing the adenylyl cyclase signalosome: sorting out the partners and the steps. Naunyn Schmiedebergs Arch Pharmacol. 2012;385(1):5–12. doi: 10.1007/s00210-011-0696-9. PubMed PMID: 22012074. [PubMed: 22012074]

23. Efendiev R, Samelson BK, Nguyen BT, Phatarpekar PV, Baameur F, Scott JD, Dessauer CW. AKAP79 interacts with multiple adenylyl cyclase (AC) isoforms and scaffolds AC5 and −6 to alpha-amino-3-hydroxyl-5-methyl-4-isoxazole-propionate (AMPA) receptors. The Journal of biological chemistry. 2010;285(19):14450–8. doi: 10.1074/jbc.M110.109769. PubMed PMID: 20231277; PMCID: PMC2863235. [PubMed: 20231277]

24. Dessauer CW. Kinetic analysis of the action of P-site analogs. Methods Enzymol. 2002;345:112–26. PubMed PMID: 11665599. [PubMed: 11665599]

25. Villar VA, Cuevas S, Zheng X, Jose PA. Localization and signaling of GPCRs in lipid rafts. Methods Cell Biol. 2016;132:3–23. doi: 10.1016/bs.mcb.2015.11.008. PubMed PMID: 26928536. [PubMed: 26928536]

26. Qiu Z, Ghosh A. A brief history of neuronal gene expression: regulatory mechanisms and cellular consequences. Neuron. 2008;60(3):449–55. doi: 10.1016/j.neuron.2008.10.039. PubMed PMID: 18995819. [PubMed: 18995819]

27. Tesmer JJ, Sunahara RK, Gilman AG, Sprang SR. Crystal structure of the catalytic domains of adenylyl cyclase in a complex with Gsalpha.GTPgammaS. Science. 1997;278(5345):1907–16. PubMed PMID: 9417641. [PubMed: 9417641]

28. Vercellino I, Rezabkova L, Olieric V, Polyhach Y, Weinert T, Kammerer RA, Jeschke G, Korkhov VM. Role of the nucleotidyl cyclase helical domain in catalytically active dimer formation. Proc Natl Acad Sci U S A. 2017;114(46):E9821–E8. doi: 10.1073/pnas.1712621114. PubMed PMID: 29087332; PMCID: PMC5699072. [PubMed: 29087332]

29. Zimmermann G, Zhou D, Taussig R. Activating mutation of adenylyl cyclase reverses its inhibition by G proteins. Molecular pharmacology. 1999;56(5):895–901. PubMed PMID: 10531392. [PubMed: 10531392]

30. Taussig R, Iniguez-Lluhi JA, Gilman AG. Inhibition of adenylyl cyclase by Gi alpha. Science. 1993;261(5118):218–21. PubMed PMID: 8327893. [PubMed: 8327893]

31. Dessauer CW, Tesmer JJ, Sprang SR, Gilman AG. Identification of a Gialpha binding site on type V adenylyl cyclase. The Journal of biological chemistry. 1998;273(40):25831–9. PubMed PMID: 9748257. [PubMed: 9748257]

32. Seifert R Vidarabine is neither a potent nor a selective AC5 inhibitor. Biochemical pharmacology. 2014;87(4):543–6. doi: 10.1016/j.bcp.2013.12.025. PubMed PMID: 24398424. [PubMed: 24398424]
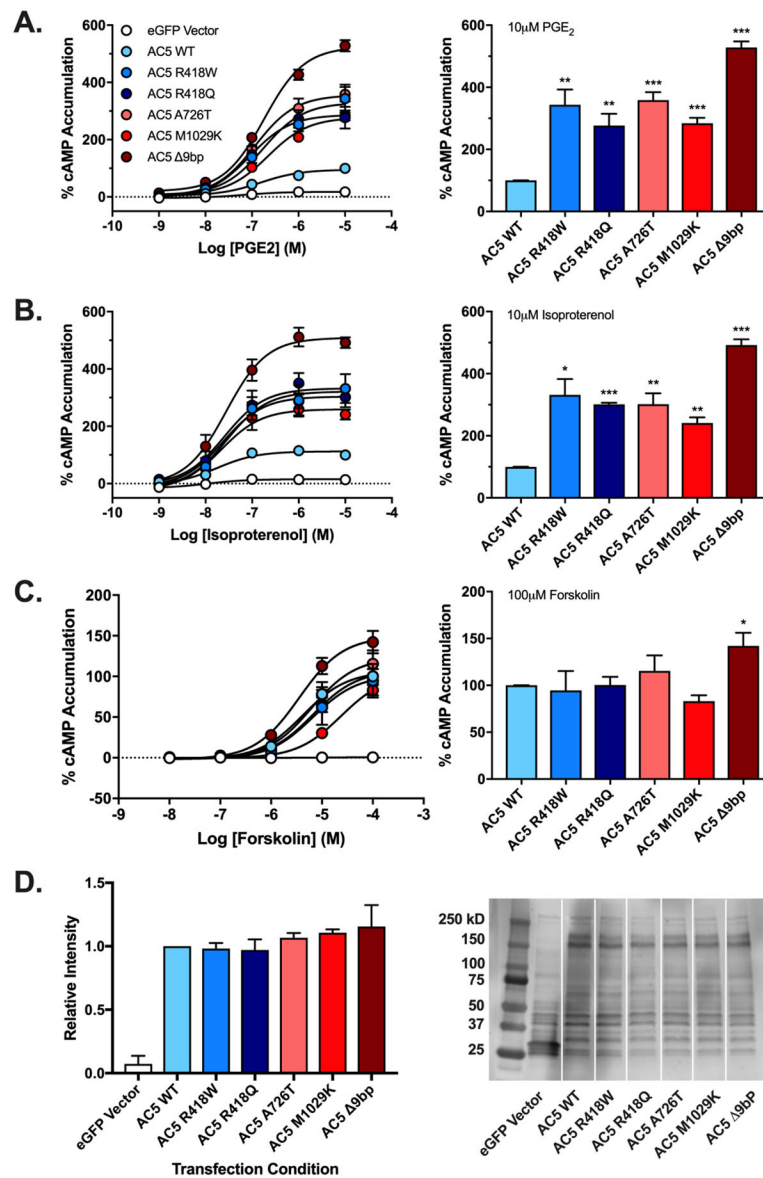
Figure 1. Gα$_s$-coupled receptor and forskolin-mediated cAMP formation by AC5 and variants
Activity of indicated AC5-eGFP fusions expressed in HEK AC3/AC6⁻ cells was measured
using CisBio HTRF cAMP assay in response to stimulation with PGE$_2$/PGER (A),
Isoproterenol/β$_2$AR (B), or FSK (C). Bar graphs represent response observed at highest
concentration stimulant tested (10 μM PGE$_2$, 10 μM Isoproterenol, 100 μM FSK). Data were
normalized to wildtype AC5, where basal activity is 0% and maximal observed activity is
100%. Data represent mean ± SEM from three individual experiments, each performed with
duplicate wells. One sample t test with Bonferroni correction was carried out for statistical
analyses. *p<0.05, ** p<0.01, ***p<0.001 all compared to AC5 wildtype. Biochemical
validation of construct expression of construct expression was carried out by Western
blotting. Whole cell fractions (D) from HEK-AC⁻3/6 cells expressing listed eGFP-AC5
construct were subject to western blot analysis using antibodies for eGFP. Data were
normalized to wildtype AC5 expression. Bar graph (left) represents relative band intensity

with representative immunoblots (right). Data represent mean ± SEM from three individual experiments, significance of construct expression determined using one sample t test with Bonferroni correction. *p<0.05, ** p<0.01, ***p<0.001 AC5 mutants compared to wildtype.
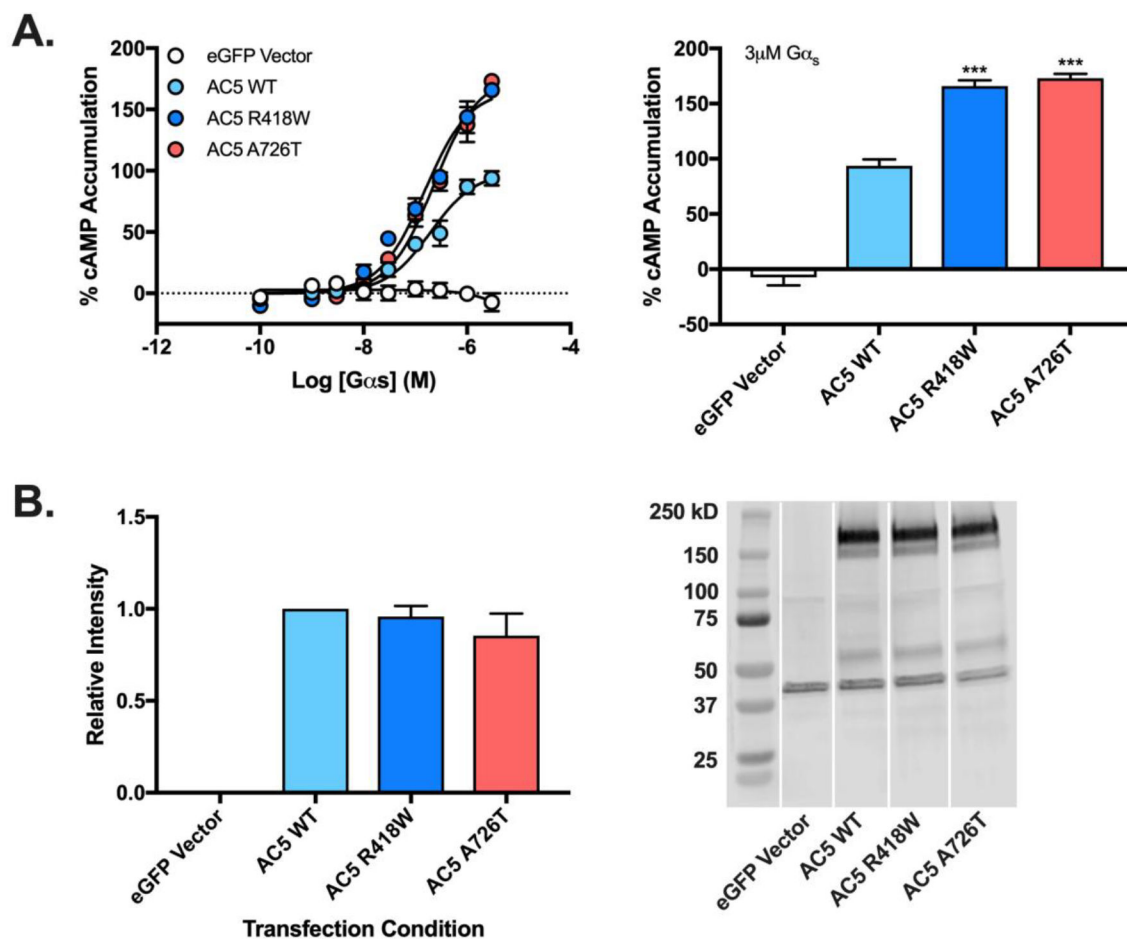
Figure 2. Stimulation of AC5 variants by recombinant Gαs-GTPγS

Membrane preparations of HEK AC3/AC6⁻ cells expressing indicated AC5 construct at 250 ng/well were stimulated using purified Gαs-GTPγS and cAMP measured using CisBio HTRF assay (A). Bar graph represent response observed at 3 μM Gαs. Data were normalized to wildtype AC5, where basal activity is 0% and maximal observed activity is 100%. Data represent mean ± SEM from three individual experiments, each performed with duplicate wells. One sample t test with Bonferroni correction was carried out for statistical analyses. *p<0.05, ** p<0.01, ***p<0.001 all compared to AC5 wildtype. Biochemical validation of construct expression of construct expression was carried out by Western blotting. Membrane fractions (B) from HEK-AC 3/6 cells expressing listed eGFP-AC5 construct were subject to western blot analysis using antibodies for eGFP. Data were normalized to wildtype AC5 expression. Bar graph (left) represents relative band intensity with representative immunoblots (right). Data represent mean ± SEM from three individual experiments, significance of construct expression determined using one sample t test with Bonferroni correction. *p<0.05, ** p<0.01, ***p<0.001 AC5 mutants compared to wildtype.
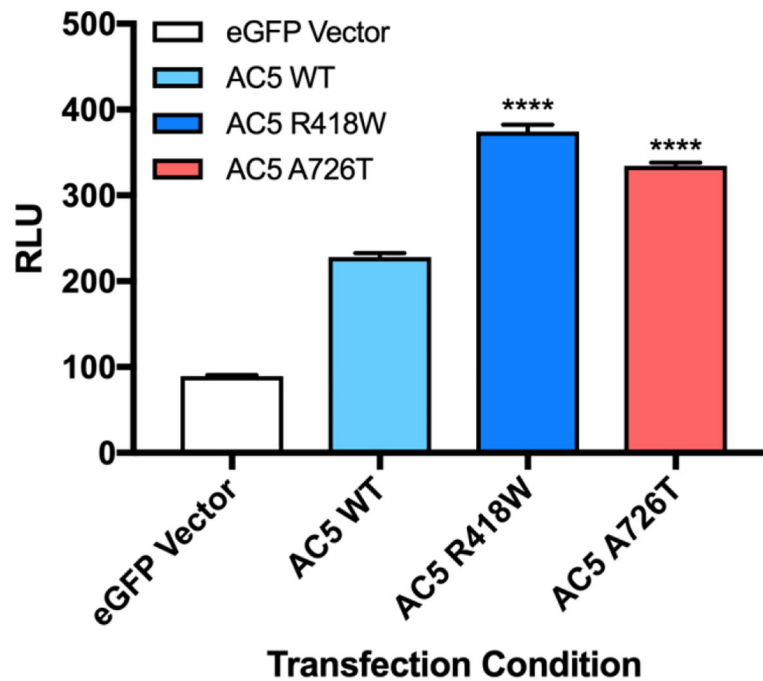
Figure 3. Evaluation of downstream cAMP signaling of AC5 variants in neuronal cell line
CRE-driven luciferase activity was measured in CAD cells transfected with indicated AC5 construct in response to stimulation with 1 μM CGS 21680 (A_2AR receptor agonist). Data presented as relative luminescence units (RLU). Data represent mean ± SEM from three individual experiments, each performed with duplicate wells. Basal CRE-driven luciferase activity was eGFP, 54 ± 2; AC5 WT, 141 ± 6; AC5 R418W, 115 ± 5; AC5 A726T, 125 ± 4. **** P 0.0001, as determined using one-way ANOVA with Dunnett's multiple comparisons test in comparison to AC5 wildtype.
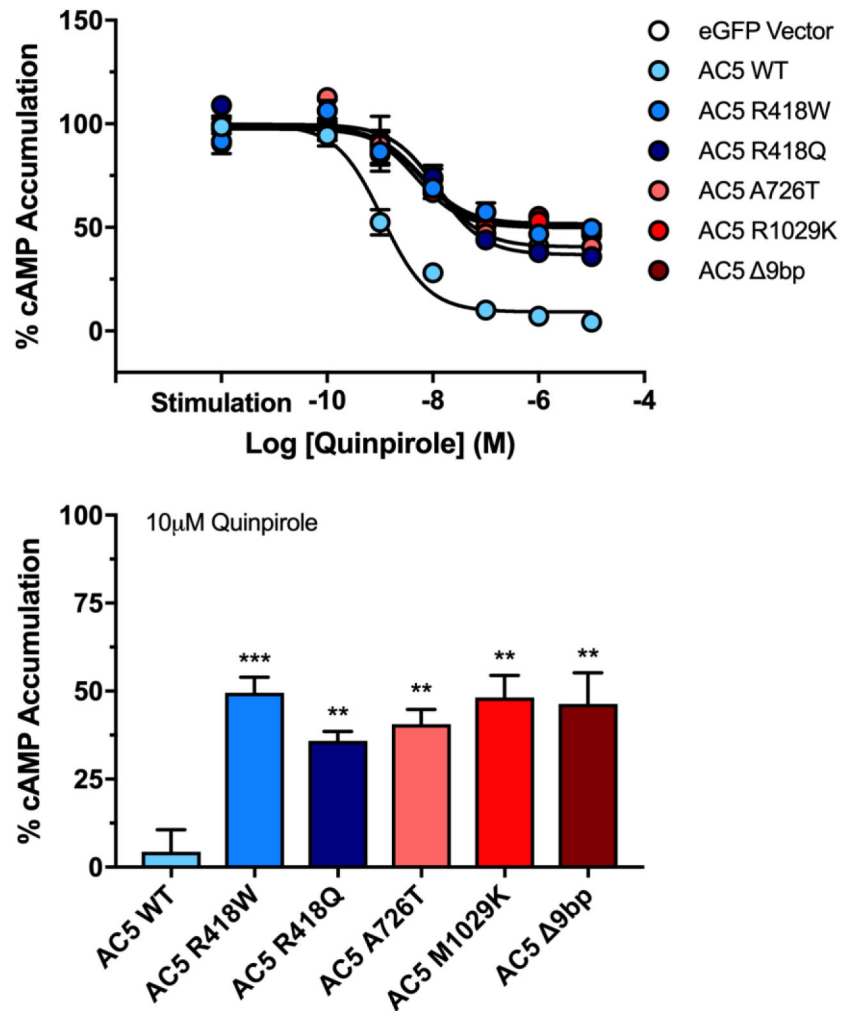
Figure 4. Gα$_{i/o}$-mediated inhibition of AC5 variants

HEK-AC 3/6 cells expressing D$_{2L}$R and indicated AC5 variant were incubated with increasing concentrations of D$_2$R agonist quinpirole, followed by stimulation with 1 μM isoproterenol. Data were normalized, where basal activity is 0% and stimulation is 100%. Stimulation represents maximal observed activity in response to 1 μM isoproterenol in the absence of quinpirole. Bar graph represents the isoproterenol response in the presence of 10 μM quinpirole. Data represent mean ± SEM from three individual experiments, each performed with duplicate wells. One sample t test with Bonferroni correction was carried out for statistical analyses. *p<0.05, ** p<0.01, ***p<0.001 all compared to AC5 wildtype.
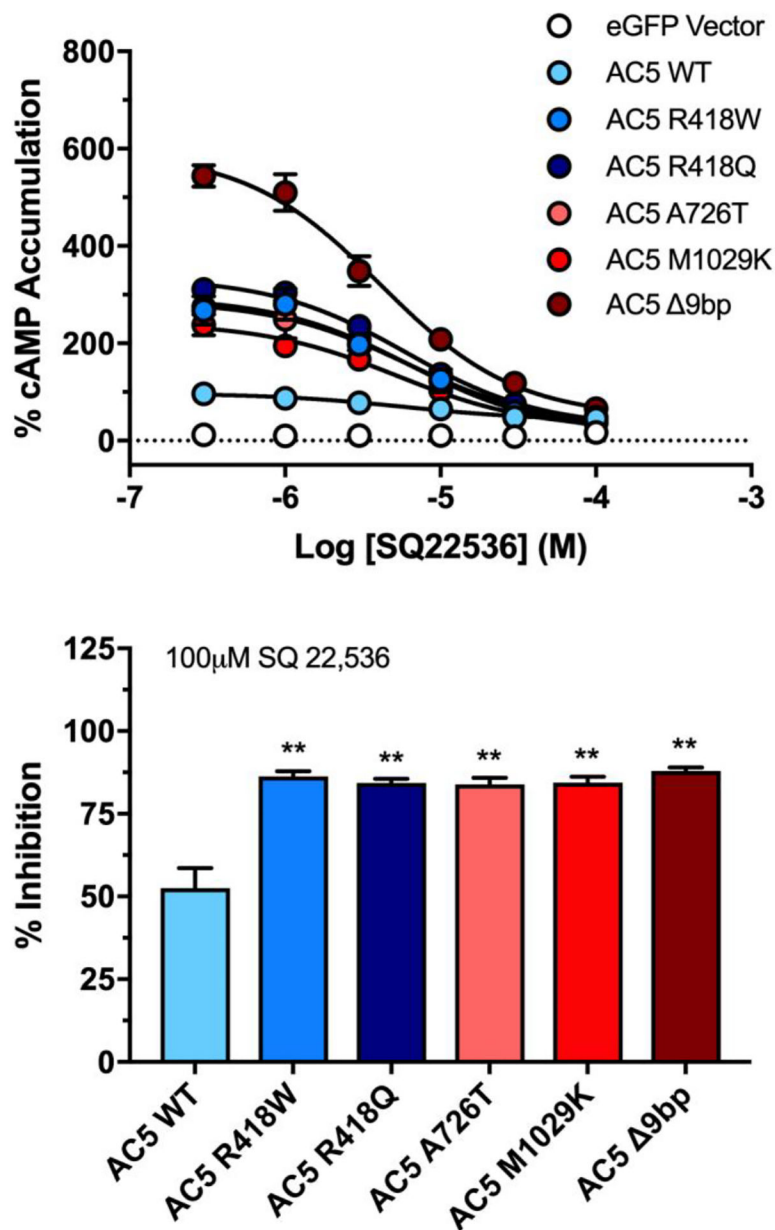
Figure 5. Inhibition of AC5 variant activity by P-site inhibitor SQ 22,536

HEK-AC 3/6 cells expressing indicated AC5 variant were incubated with increasing concentrations of P-site inhibitor SQ 22,536, followed by stimulation with 1 μM isoproterenol. Data were standardized to wildtype AC5, where basal activity is 0% and maximal observed activity in the absence of inhibitor is 100%. Bar graph represents % inhibition of stimulation following treatment with 100 μM SQ 22,536. Data represent mean ± SEM from three individual experiments, each performed with duplicate wells. One sample t test with Bonferroni correction was carried out for statistical analyses. *p<0.05, ** p<0.01, ***p<0.001 all compared to AC5 wildtype.
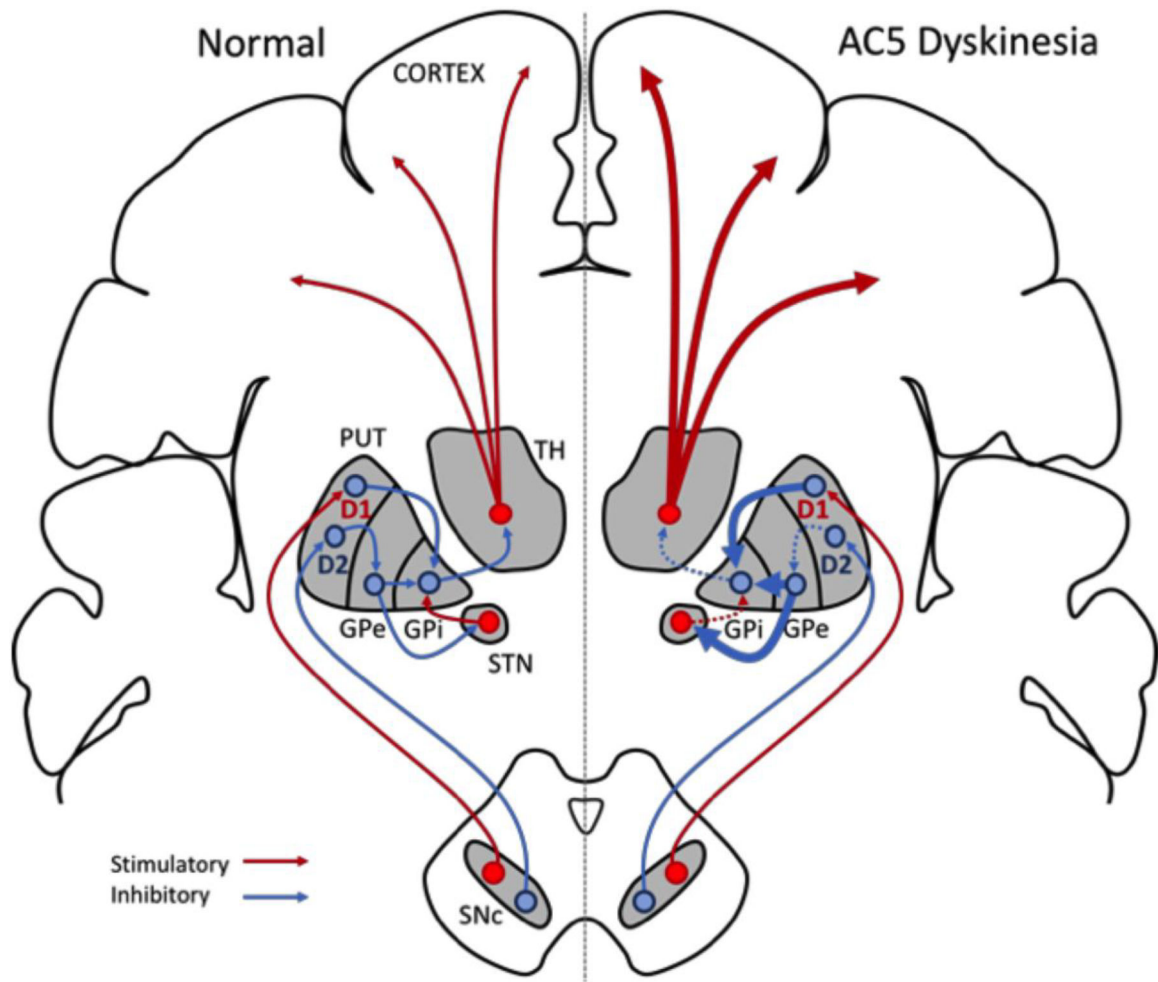
Figure 6. Pathway model of AC5 variant effects

A schematic model of normal basal ganglia signaling (left) versus that possibly observed in AC5-related dyskinesia (right). As previously described, AC5 is the principal adenylyl cyclase isoform expressed in the striatum, and preferentially couples to both D_1 and D_2 dopamine receptors. Our results suggest that the enhanced activity observed following $G\alpha_s$-mediated stimulation of AC5 gain-of-function mutations may lead to increased direct pathway activity. Furthermore, the observation that AC5 gain-of-function variants are weakly inhibited by D_2 receptor activation suggest that decreased activity of the indirect pathway may be observed. Together, this loss of cooperative activity in both direct and indirect pathways may possibly result in the unsynchronized enhancement of movement initiation observed in AC5-associated dyskinesia resulting from gain-of-function variants.

Table 1.

Effects of receptor-mediated stimulation and inhibition of AC5 and variants

Cyclase	PGE2		Isoproterenol		Forskolin		Quinpirole		SQ 22,536	
	Max %	EC50 (nM)	Max %	EC50 (nM)	Max %	EC50 (µM)	Max %	IC50 (nM)	Max %	IC50 (µM)
AC5 WT	100	151 (88–282)	100	18 (7–42)	100	4 (3–7)	96 ± 4	1 (1–2)	53 ± 6	6 (2–18)
AC5 R418W	343 ± 49	173 (63–595)	332 ± 51	29 (9–98)	95 ± 21	7 (1–30)	50 ± 3	6 (2–23)	86 ± 2	6 (3–14)
AC5 R418Q	277 ± 38	91 (35–226)	301 ± 5	25 (9–74)	100 ± 9	7 (4–12)	64 ± 2	12 (6–26)	84 ± 1	6 (4–9)
AC5 A726T	359 ± 25	118 (65–221)	302 ± 35	24 (11–54)	115 ± 17	6 (2–15)	59 ± 2	12 (5–26)	84 ± 1	6 (2–16)
AC5 M1029K	284 ± 17	220 (117–445)	241 ± 18	22 (9–57)	83 ± 6	24 (15–41)	52 ± 4	5 (2–10)	84 ± 2	5 (3–9)
AC5 9bp	528 ± 20	182 (129–262)	492 ± 19	28 (14–55)	142 ± 14	4 (2–6)	54 ± 5	6 (2–23)	88 ± 1	4 (3–7)

Biochemical characterization of AC5 and variants in response to receptor and small molecule-mediated stimulation in intact HEK-AC 3/6 cells using Cisbio HTRF cAMP assay. Data represent the mean maximal efficacy (Max%) with SEM from $n = 3$ independent experiments, each with duplicate wells. EC50 and IC50 data are listed with 95% CI in parentheses.